CrossMark

ORIGINAL CONTRIBUTION

The vesicle formation of β-CD and AD self-assembly of dumbbell-shaped amphiphilic triblock copolymer

Lujuan Xu[1] · Xinyi Liang[1] · Lin Zhang[1] · Jinbi Wu[1] · Zhanxian Li[1] · Mingming Yu[1] · Liuhe Wei[1]

Abstract Vesicles of a noncovalent dumbbell-shaped amphiphilic triblock copolymer were formed by self-assembly of host-guest inclusion between β-cyclodextrin containing poly(ethylene oxide) (β-CD-PEO) and adamantyl group containing polystyrene (AD-PS-AD) in solution. Addition of water into the copolymer resulted in the formation of new bowl-shaped and vesicle morphologies by adjusting not only ratio of solvents (THF dioxane or DMF) but also the length of the PS middle block in the guest polymer, which was ascribed to the large compound micelles (LCMs). The continuous phase of PS was composed of an assembly of reversed micelles (PEO core and PS corona) with hydrophilic PEO chains surrounding the structure at the polymer/aqueous solution interface in the larger compound micelles.

Electronic supplementary material The online version of this article (doi:10.1007/s00396-015-3758-6) contains supplementary material, which is available to authorized users.

✉ Mingming Yu
yumm@zzu.edu.cn

✉ Liuhe Wei
weiliuhe@zzu.edu.cn

[1] College of Chemistry and Molecular Engineering, Zhengzhou University, Zhengzhou 450001, China

Introduction

Supramolecular polymers can be formed as various microstructures [1–3] and have been observed in a range of areas, e.g., associative thickener nanoparticles [4], gene carriers [5, 6], and biosensing devices [7, 8]. Different intermolecular interactions of polymer-polymer associations have been used such as hydrophobic interactions occurring in aqueous systems of amphiphilic copolymers, electrostatic interactions between polymers with opposite charges [9], interprotein heme-heme pocket binding [10, 11], hydrogen bond interactions in proteins [12, 13], and inclusion complexes with β-cyclodextrin compounds [14–20].

Cyclodextrins (CDs) are a series of natural cyclic oligomers composed of six, seven, or eight α-1,4-linked D-glucose units and named α-, β-, or γ-CD, respectively [21]. Shaped as a hollow truncated cone, cyclodextrin (CD) has a hydrophilic exterior and a hydrophobic inner cavity with a depth of ca. 7.0 Å and an internal diameter of ca. 4.5, 7.0, and 8.5 Å for α-, β-, and γ-CD, respectively. Various molecules can be fitted into the cavities to form "guest-host" inclusion complexes. For instance, the adamantyl group fits into the β-cyclodextrin cavity precisely [22] and the association constants for the inclusion complex are 10^4–10^5 [23].

The so-called "dumbbell" polymer has a linear central block which connects two star branched ends and each chain end has five or more arms [24, 25]. Synthesis of the dumbbell-shaped block polymers were reported using reversible addition–fragmentation transfer (RAFT) reaction [26, 27], copper-mediated atom transfer radical polymerization (ATRP) [28], and difunctional poly(n-BA) macroinitiator [29]. Here, we reported the synthesis of a noncovalent dumbbell-shaped amphiphilic triblock copolymer which was prepared through the host-guest inclusion between β-cyclodextrin containing poly(ethylene oxide) and the adamantane-polystyrene-adamantane.

Amphiphilic triblock copolymers, when dissolved in a selective solvent that is good for one block and poor for the other, can self-assemble into a variety of micellar structures, such as spheres, vesicles, rod-like micelles, and bowl-shaped structure [30]. The self-assembly of amphiphilic triblock copolymers shows interesting solution behavior, suggesting their potential applications in drug delivery systems and biological vectors [31–37]. Noncovalent interactions have successfully been applied to build supramolecular polymers [38–41]. To date, noncovalent amphiphilic triblock copolymers have rarely been reported.

Recently, aggregates of various morphologies have been observed in a number of self-assembled systems [42–48]. Spherical micelles have been observed frequently in solutions of block copolymers [49–51]. Micelles with non-spherical morphologies are usually detected by indirect methods for the relative composition of the blocks, such as light scattering [52, 53], SAXS [54]. Sometimes, amphiphilic poly(ethylene-*alt*-propylene)-poly(ethylene oxide) diblock copolymer in aqueous solutions can yield "crew-cut" type micelle [55]. The aggregates are called crew-cut because the dimensions of the core are much larger than those of corona, as opposed to the star micelles [56], where the core is small and the corona is relatively large. The copolymer was first dissolved in a common solvent for both blocks and then water was added as a precipitant to the solution to induce segregation of the long hydrophobic segments. When the water was added, the quality of the solvent for the long block was reduced. The aggregation of the hydrophobic segments emerged when content of water reached the critical water content (CWC). The morphology of the aggregates could be observed in water.

The "crew-cut" aggregates of amphiphilic block copolymer in selective solvents have attracted increasing interest for their industrial and scientific significance. The previous reports have explored extensively the preparation and observation of "crew-cut" aggregates of various morphologies from highly asymmetric diblock copolymer such as polystyrene-*b*-poly(ethylene oxide) (PS-*b*-PEO) polybutadiene-*b*-poly(2-vinylpyridine) (PB-*b*-P2VP) [53], poly(styrene-*b*-4-vinylpyridine) (PS-*b*-P4VP) [57], polystyrene-*b*-polyisoprene (PS-*b*-PI) [58, 59], polystyrene-*b*-poly(acrylic acid) (PS-*b*-PAA) [60], and poly(ethylene oxide)-*block*-poly(*n*-butylacrylate) (PEO-P*n*BA) [61]. There are rare reports on the "crew-cut" aggregates of noncovalent dumbbell-shaped amphiphilic triblock copolymers.

This paper describes the preparation of an additional non-equilibrium morphology of crew-cut aggregates, consisting of a dumbbell-shaped structure, prepared from the host-guest inclusion between β-cyclodextrin containing poly(ethylene oxide) (β-CD-PEO) and the adamantane-polystyrene-adamantane (AD-PS-AD). The formation mechanism was proposed based on one previously encountered crew-cut structure from 5-(*N,N,N*-diethylmethylammonium)isoprene and styrene triblock copolymers (PAI-*b*-PS-*b*-PAI). It is suggested that the dumbbell-shaped structure is kinetically controlled.

Experimental

Materials

Ph$_3$P (99 %), CuBr (99.5 %), 2,2′-dipyridine (99.7 %), THF (AR), styrene (99 %), β-cyclodextrin (98 %), Na (98 %), and CuSO$_4$•5H$_2$O (98 %) were purchased from Sinopharm Chemical Reagent Co. Ltd. *N,N*-Dimethyl formamide (AR), tetrahydrofuran (AR), methanol (AR), and pyridine (chemical pure) were purchased from Tianjin Chemical Reagent Plant No. 1. 2-Bromoisobutyryl bromide (98 %) and 1-adamantanecarboxylic acid chloride (97 %) were purchased from Alfa Aesar and used as received. *N,N*-Dimethyl formamide (DMF) was dried over 4A molecular sieve overnight and distilled under reduced pressure before use. Pyridine and triethylamine (TEA) were dried over CaH$_2$ and distilled. Tetrahydrofuran (THF) was distilled from a solution containing the Na/Ph$_2$CO ketal. Ethyl ether was dried over MgSO$_4$ and then filtered. Styrene was washed with 1 M aqueous NaOH to remove the inhibitor and then with water, dried over anhydrous MgSO$_4$ and distilled over CaH$_2$ under reduced pressure before use. CuBr was purified by stirring in acetic acid. After filtration, it was washed with 2-propanol and then dried in vacuum.

Methods

FT-IR spectra were recorded on a NEXUS-470 spectrometer at frequencies ranging from 400 to 4000 cm^{-1}. Samples were thoroughly mixed with KBr and pressed into pellet form. ^{1}H NMR spectroscopy was performed on a DRX-400 spectrometer. Tetramethylsilane was used as an internal standard. The apparent molecular weights and polydispersities (Mw/Mn) of linear polymers were determined on an Agilent LC 1200 gel permeation chromatograph (GPC) equipped with Agilent PL columns, a refractive index detector at 38 °C, and THF was used as the eluent (1.0 mL/min). Transmission electron microscopy (TEM) was carried out with a JEM-2010/INCA OXFORD TEM (JEOL/OXFORD) at a 200-kV accelerating voltage. Samples were deposited onto the surface of 300 mesh Formvar-carbon film-coated copper grids. Excess solution was quickly filtered out with a filter paper. Scanning electron microscopy (SEM) images were recorded using a JSM-7500 F field-emission microscope, and the samples were prepared by drop-casting an aqueous solution of aggregates onto a copper grid.

Synthesis of per-6-iodo-β-cyclodextrin

Ph$_3$P (40.1 g, 153 mmol) was dissolved in dry DMF (160 mL). I$_2$ was carefully added (40.5 g, 160 mmol) to this solution over 10 min with the evolution of heat: the solution reached 50 °C. Dry β-cyclodextrin (11.6 g, 10.2 mmol) was then added to this dark brown solution, and the temperature was raised to 70 °C. At this temperature, the solution was stirred under an atmosphere of Ar for 18 h. The solution was concentrated under reduced pressure to remove DMF (approximately 100 mL). NaOMe in MeOH (3 M, 70 mL) was then prepared by adding Na (5.6 g) to MeOH (60 mL) under an inert atmosphere with efficient cooling. This NaOMe solution was added to the reaction vessel with cooling, and the reaction mixture was stirred for 30 min. The following reaction deviated from the literature procedure. Instead of precipitating the product with ice-water, the reaction mixture was poured into MeOH (80 mL) to form a precipitate, which was washed with MeOH, superficially dried, and then Soxhlet extracted with MeOH for 24 h until no more discoloration of the solvent could be detected. The product was removed from the Soxhlet extractor and allowed to air dry before being dried under high vacuum. The synthetic compound (17.9 g, 90 %) was gained as a white powder. ^{1}H NMR (400 MHz, CD$_3$SOCD$_3$, δ): 3.28 (t, 7 H) 3.34–3.48 (m, 14 H), 3.54–3.68 (m, 14 H), 3.80 (d, 7 H), 4.99 (d, 7 H), 5.94 (d, 7 H), 6.05 (d, 7 H); ^{13}C NMR (100 MHz, CD$_3$SOCD$_3$, δ): 71.0, 72.0, 72.3, 86.0, 102.2.

Synthesis of per-6-azido-β-cyclodextrin

Per-6-iodo-β-cyclodextrin (2.99 g, 1.57 mmol) was dissolved in DMF (50 mL), and NaN$_3$ (1.00 g, 15.4 mmol) was added. The resulting suspension was stirred at 60 °C under an atmosphere of Ar for 20 h. The suspension was then concentrated under reduced pressure to a few milliliters before a larger excess of H$_2$O was added. A fine white precipitate was formed and was filtered off carefully. The precipitate was washed with H$_2$O and dried under high vacuum to yield a stable white powder. Per-6-azido-β-cyclodextrin (2.01 g, 98 %) was obtained. IR (KBr, cm^{-1}): 3357 cm^{-1} (OH), 2107 cm^{-1} (-N$_3$); ^{1}H NMR (400 MHz, CD$_3$SOCD$_3$, δ): 3.30–3.42 (m, 14 H), 3.53–3.65 (m, 14 H), 3.68–3.82 (m, 14 H), 4.91 (d, 7 H), 5.77 (d, 7 H), 5.92 (d, 7 H).

Synthesis of acetylated-per-azido-β-cyclodextrin

Acetic anhydride (90.0 mL) was added to a solution of per-6-azido-β-cyclodextrin (12.0 g, 9.20 mmol) in dry pyridine (86.0 mL) and stirred at 50 °C under an atmosphere of Ar for 12 h. The solution was then concentrated and the residue was dissolved in CH$_2$Cl$_2$ (250 mL) and washed with 10 % HCl (2 × 100 mL) followed by water (2 × 100 mL). The organic layer was dried over Na$_2$SO$_4$ and concentrated to yield a crude

orange product. The crude product was purified via silica gel column chromatograph using benzene:ethanol (16:1) as the eluent. The proper fractions were collected and concentrated yielding acetylated-per-azido-β-cyclodextrin (12.5 g, 70 %). ^{1}H NMR (400 MHz, CD$_3$SOCD$_3$, δ): 2.08 (s, 21 H), 2.10 (s, 21 H), 3.60–3.80 (m, 21 H), 4.00–4.10 (m, 7 H), 4.81 (d, 7 H), 5.09 (d, 7 H), 5.29 (t, 7 H).

Synthesis of alkyne poly(ethylene oxide)

NaH (1.00 g of 60 % suspension in oil, 25 mmol) was added to a THF solution (30 mL) of PEO (3.5 g, 10 mmol) at 0 °C. The mixture was stirred at 0 °C for 30 min and then at room temperature for 30 min followed by the addition of propargyl bromide (3.45 g, 29 mmol) under argon atmosphere. After 6 h, the resulting solution was extracted with water (2 × 50 mL) and then HCl solution was added into the water layer until it showed acidity. The water layer was extracted with CH$_2$Cl$_2$ (2 × 50 mL), and CH$_2$Cl$_2$ was removed under reduced pressure to give the product alkyne poly(ethylene oxide) (3.70 g, 95 %). ^{1}H NMR (400 MHz, CDCl$_3$, δ): 2.5 (1 H), 3.4 (3 H), 3.5–3.8 (35 H), 4.2 (2 H), ^{13}C NMR (100 MHz, CD$_3$SOCD$_3$, δ): 59, 69, 70, 75, 80. IR (KBr, cm^{-1}): 3245.69 (C-H), 2112.47 (alkynyl), 1104.96 (C-O-C).

Synthesis of protecting "click" copolymers (acetylated-β-CD-PEO)

Acetylated-per-azido-β-cyclodextrin (69.5 mg, 1.09 × 10^{-4} mol) and alkyne poly(ethylene oxide) (29.4 mg, 1.55 × 10^{-5} mol) were dissolved in 2.6 mL 1:1 THF/water solution. Fresh solution of 1 M CuSO$_4$•5H$_2$O and 1 M sodium ascorbate were prepared and used to introduce the catalyst 5 % CuSO$_4$ and 10 % sodium ascorbate to the reaction to promote the click coupling reaction. This mixture was stirred at 60 °C for 24 h. The reaction mixture was then extracted with dichloromethane (2 × 50 mL). The dichloromethane layer was concentrated by rotary evaporation and then dried under high vacuum to give the compound acetylated-β-CD-PEO (60 %). IR: (KBr, cm^{-1}): 2872.42, 1670.34, 1388.58, 1066.80. ^{1}H NMR (400 MHz, D$_2$O, δ): 2.52 (H), 3.41 (3 H), 3.52–3.83 (35 H), 4.22 (2 H), 3.94–5.09 (m, 49 H, cyclodextrin protons), 8.06 (s, 7 H, triazole).

Synthesis of deprotected "click" chemical compound (β-CD-PEO)

The acetate groups were deprotected by conventional methods. In brief, 250 mg protected click compound acetylated-β-CD-PEO was dissolved in 5 mL anhydrous methanol. The acetate groups were first deprotected by adjusting the pH to 9 using solid sodium methoxide and stirring the resulting solution overnight. The product was

dialyzed against methanol, concentrated and dried in vacuum. The resulting solid was then dissolved in 10 mL HCl/dioxane and stirred at room temperature for 3 h. The solution was concentrated to yield the crude product. IR: (KBr pellet, cm^{-1}): 3446.41, 2872.42, 1670.34, 1388.58, 1066.80. ^{1}H NMR (400 MHz, D$_2$O, δ): 2.52 (H), 3.41 (3 H), 3.53–3.82 (35 H), 4.2 (2 H), 3.94–5.09 (m, 49 H, cyclodextrin protons), 3.10–3.34 (t, 49 H, CH$_2$ and H-4), 3.52 (s, 7 H, H-2), 3.89–3.93 (t, 7 H, H-3), 4.07–4.14 (s, 14 H, H-5), 4.42–4.59 (s, 7 H, H-6), 5.05 (s, 7 H, H-1), 8.06 (s,7 H, triazole).

Synthesis of Br-benzene-Br initiator

In a typical example, hydroquinone (0.135 g, 1.2 mmol) was dissolved in 100 mL THF in a three-neck flask. After azeotropic distillation of 50 mL THF at reduced pressure to remove trace amount of water, triethylamine (1.7 mL, 0.012 mol) was added and the solution mixture was cooled to 0 °C. Then, 2-bromoisobutyryl bromide (1.5 mL, 0.012 mol) was added dropwise for 1 h and the reaction mixture was stirred at room temperature for 48 h. The precipitate of the stirred solution was removed by filtration. The filtrate was concentrated under reduced pressure, precipitated in water, and dried under high vacuum. ^{1}H NMR (400 MHz, CDCl$_3$, δ): 2.01 (s, 12 H), 7.12 (s, 4 H).

Synthesis of polystyrene containing terminal azido group (N$_3$-PS-N$_3$)

The test tube containing initiator (0.204 g, 0.5 mmol), styrene (3.4 mL, 3 mmol), CuBr (0.072 g, 0.5 mmol), and bipyridyl (0.156 g, 1 mmol) was degassed using 3 freeze/pump/thaw cycles. Upon thawing, the reaction test glass was placed in a preheated 110 °C oil bath and allowed to stir under argon for 90 min. The reaction mixture was then cooled to room temperature and dissolved in THF. After passing through a column of Al$_2$O$_3$ gel, precipitation from methanol gave the Br-PS-Br. Then, Br-PS-Br (0.239 g, 4.1×10^{-5} mol) was dissolved in DMF (3 mL) and sodium azide (0.013 g, 2.0×10^{-4} mol) was added. The reaction mixture was allowed to be stirred for 20 h and purified by precipitation from methanol. ^{1}H NMR (400 MHz, CDCl$_3$, δ): 2.01 (s, 12 H), 7.12 (s, 4 H), 6.21–7.22 (aromatic protons).

Synthesis of alkyne 1-adamantane

Anhydrous pyridine (3.5 mmol) was added to a solution of 1-adamantanecarboxylic acid chloride (0.600 g, 3 mmol) and propargyl alcohol (0.280 g, 3 mmol) in 70 mL absolute diethyl ether. The mixture was slightly shaken and allowed to stay at 20 °C for 24 h. The precipitate of pyridine hydrochloride was filtered and washed with 30 mL diethyl ether; the combined filtrate was washed with water and saturated aqueous solution of sodium hydrogen carbonate. The ether solution was dried over CaCl$_2$, the solvent was distilled off, and the residue was dried in vacuum to give alkyne 1-adamantane. ^{1}H NMR (400 MHz, CD$_3$SOCD$_3$, δ): 1.61 (6 H), 1.92 (6 H), 2.12 (3 H), 2.51 (1 H), 4.71 (2 H).

Synthesis of host-guest inclusion between β-cyclodextrin containing poly(ethylene oxide) (β-CD-PEO) and adamantane-polystyrene-adamantane (AD-PS-AD)

β-Cyclodextrin containing poly(ethylene oxide) polymer was dissolved in THF, then adamantane-polystyrene-adamantane was added with a 1/1 molar ratio of adamantane/cyclodextrin. After water (the same volume as THF) was added, the resulting mixture was mixed vigorously in ultrasound to form a homogeneous solution for 6 h. The resulting complex was concentrated under reduced pressure and then dried under high vacuum.

Synthesis of adamantane-polystyrene-adamantane compound (AD-PS-AD) via click chemistry

A typical procedure for the synthesis of AD-PS-AD compounds was started with a 1/0.9/1/1 molar ratio of reagents alkyne AD/N$_3$-PS-N$_3$/CuBr/PMDETA. The click coupling reaction between alkyne AD (6.21 mg, 0.03 mmol) and N$_3$-PS-N$_3$ (0.52 g, 0.02 mmol) was conducted at 60 °C in a 25-mL Schlenk flask with 2 mL DMF as solvent and CuBr/PMDETA as catalyst. After 24 h, the polymer solution was then precipitated in methanol. The precipitate was washed with methanol, filtered off, and then dried under vacuum at 40 °C to give 158.51 mg triblock copolymers AD-PS-AD (69.5 %). ^{1}H NMR (400 MHz, CD$_3$SOCD$_3$, δ): 1.61–2.12 (adamantane protons), 6.21–7.22 (aromatic protons).

Synthesis of self-assembled nanoparticles from PEO-β-CD-AD-PS-AD-β-CD-PEO copolymers in aqueous solution

A typical procedure for the preparation of PEO-β-CD-AD-PS-AD-β-CD-PEO nanoparticles was as follows: 0.012 g PEO-β-CD-AD-PS-AD-β-CD-PEO sample was dissolved completely in 2 mL THF at room temperature, and then distilled water was added dropwise to the resulting solution (0.006 g/mL) under vigorous stirring using a microsyringe. The solution was stirred vigorously for another 48 h at room temperature, and THF was completely removed by dialysis. The copolymer nanoparticles formed by self-assemble method (Scheme 1).
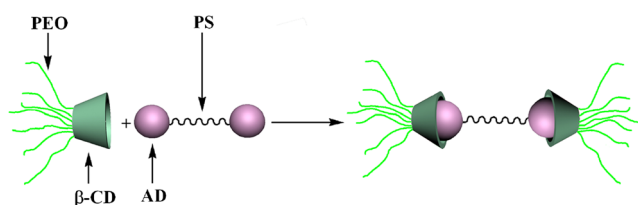
Scheme 1 Schematic representation of the inclusion complexes formed through host-guest interaction between β-CD and AD

Results and discussion

Synthesis of click reactions

The carbohydrate core, acetylated per-β-azido-cyclodextrin was synthesized using a combination of previously reported methods (Scheme S1) and a novel series of alkyne PEO containing a terminal acetylene group was designed (Scheme S1A). The IR spectrum of the compound alkyne poly(ethylene oxide) showed a characteristic peak at 3245 ($\equiv$C-H stretching) and 2112 cm^{-1} (C$\equiv$C stretching) (Fig. S1B). The key step in the synthesis of the deprotected "click" chemical compounds was carried out via click reaction, which promoted regiospecific coupling in high yield even in sterically hindered environment. As shown in Scheme S1A, the 1,3-dipolar cycloaddition of azide (4) and alkyne (5) was carried out using copper sulfate/sodium ascorbate in 1:1 THF/H$_2$O to yield the target click compounds containing the regiospecific 1,2,4-triazole, verified via ^{1}H NMR spectroscopy (Fig. S2) in 70 % yield. Because the β-cyclodextrin hydroxyl moieties are protected, copper from the catalyst and retention in the final compound was not found. Acetyl groups on the click product were deprotected via afforded conventional methods. β-Cyclodextrin click compounds (6) were purified via exhaustive dialysis in ultra pure water. The final compounds (7) were identified using ^{1}H NMR and IR spectroscopy. As shown in Figs. S2 and S3, the ^{1}H NMR showed the presence of the 1,4-triazole proton around 8.0 ppm, which indicated the success of the click reaction.

Synthesis and characterization of the click copolymers

Using ATRP, styrene (St) was polymerized with CuBr catalyst and bipyridyl ligand at 90 °C after three orders of freeze-pump-thaw cycles to remove oxygen from the reaction environment. The resulting polymer was cooled to room temperature and dissolved in THF. After passing through a column of Al$_2$O$_3$ gel to remove the copper salt, the crude product was precipitated into methanol. Via reaction with NaN$_3$ in DMF, bromine groups transformed into azido groups. Final product was characterized by ^{1}H NMR spectroscopy and Mn ranging between 4000 and 10,000 with different polydispersity (PDI< 1.49) (Table 1 and Fig. S3). Signals from 6.2 to 7.2 ppm that are characteristic peaks of protons related to benzyl groups of polystyrene.

Alkyne 1-adamantane (9) was synthesized by 1-adamantylcarbonyl chloride with propargyl alcohol in diethyl ether and pyridine at 20 °C for 24 h, in yield 70 %. The ^{1}H NMR spectra of AD-terminal alkyne group contain multiplets at 1.64 (6 H), 1.92 (6 H), 2.15 (3 H), 2.52 (1 H), and 4.74 ppm (2 H). Then the click copolymer (10) was synthesized by coupling AD- alkyne and N$_3$-PS-N$_3$ (8), verified via ^{1}H NMR spectroscopy and GPC (Figs. S3 and S4).

The characterization of dumbbell-like polymers

ROESY ^{1}H NMR spectrum confirmed the structure of the inclusion complex of β-CD-PEO moiety with PS-AD-PS moiety. Figure 1 illustrated the ROESY ^{1}H NMR spectrum of mixture β-CD-PEO polymer (5 mM) and PS-AD-PS (5 mM) in D$_2$O. The NOE cross-peaks between the signals at $\delta = 3.01$–4.02 ppm were ascribed to the interior protons of β-CD and the signals at $\delta = 1.51$–2.22 ppm were due to AD, indicating that the AD groups fell deeply into the cavities of β-CD.

The successful synthesis of dumbbell-like triblock copolymer was proved by GPC chromatogram of self-assembly complex from a 2:1 mixture of β-CD-PEO and AD-PS-AD moieties. Number-average molecular weight of peak a is 22,800 with a narrow polydispersity 1.12, which is ascribed to the dumbbell-shaped triblock copolymer. Number-average molecular weight of peak b is 4800 with a narrow polydispersity 1.16, which is attributed to AD-PS-AD (Fig. S5). NMR, IR, and GPC analysis proved the successful synthesis of triblock copolymer PEO-β-CD-AD-PS-AD-β-CD-PEO in two steps.

Aggregation behavior in selective solvent

The crew-cut structures were observed in aqueous solution of triblock copolymer PEO-β-CD-AD-PS-AD-β-CD-PEO. To our knowledge, there are few reports on the crew-cut aggregates of amphiphilic noncovalent triblock copolymers. The preparation method was copolymer dissolution in THF at room temperature, followed by the addition of water.

Two types of copolymers with different molecular weights but with approximately the same composition were investigated. The relevant data for the triblock copolymer are summarized in Table 2.

The morphologies of the bowl-shaped aggregates were prepared from the triblock copolymer 1 (Table 2) by changing the copolymer concentration in the initial THF solution. The 0.5 wt.% copolymer concentration in the initial THF solution was first investigated. TEM analysis revealed the triblock copolymer 1 formed bowl-

Table 1 Number-average molecular weight (Mn) and polydispersity index (PDI=Mw/Mn)

	Entry	Time (min)	Temp (°C)	Mw/Mn	Mn
2-Bromoisobutyryl derivative	1	80	110	1.40	9200
	2	70	110	1.49	10,000
	3	120	110	1.15	5700
	4	70	110	1.18	8300
	5	60	110	1.17	10,100
	6	70	110	1.11	3900
α,α'-Dibromo-p-xylene	7	90	110	1.27	4600
	8	90	110	1.18	7100
	9	300	110	1.38	9300
	10	300	110	1.30	11,000
	11	300	110	1.21	13,000

shaped aggregates with diameters varying from 200 to 600 nm. The image of the bowl-shaped aggregate was shown in Fig. 2. The TEM and SEM images shown in Figs. 3 and 4 show the formation of a peculiar spherical morphology with a void near the surface. The feature of these nanoparticles is the presence of cavities on the surface of the sphere, similar to the bowl-shaped aggregates reported by Eisenberg group [62, 63]. As the copolymer concentration of the triblock copolymer 2 in initial THF solution was 0.6 wt.%, the sample also formed bowl-shaped aggregates with diameters of 200–600 nm.

^{1}H NMR spectra of polymer in which α,α'-dibromo-p-xylene was employed as initiator is very similar to that in which hydroquin and 2-bromoisobutyryl bromide were use as raw materials (Scheme S2). The molar mass and polydispersity are summarized in Table 1. These two initiators belong to the same type, the influence of two different initiators is not obvious in number-average molecular weight (Mn) and polydispersity index (PDI=Mw/Mn).

The effect of the PEO block length on morphologies was also investigated. The triblock copolymer 1 has the same length of PS as copolymer 2 but a shorter PEO block. Subsequently, we studied the aggregates of several different morphologies obtained from copolymer 2 wherein the variances of the copolymer 2 concentrations in initial THF solution were accordance with those of copolymer 1 for convenient comparison. The normal spherical micelles with average diameters of 50 nm appeared in each of the samples and the bowl-shaped aggregates with an average diameter of 333 nm.

Critical aggregate concentrations (CACs) of the copolymers were estimated by a fluorescence spectroscopic method using pyrene as the fluorescence probe at 25 °C. The pyrene entered the hydrophobic core from water when the critical aggregation concentration was achieved. The final concentration of pyrene in each flask was 1.25×10^{-6} mg/mL. The excitation spectra of pyrene were obtained on a 920 Steady state/Life time Fluorescence Spectrometer, excited at 335 nm with the emission wavelength at 384 nm. The value of CAC (0.02 mg/mL) was determined from the plots of the intensity at 373 and 384 nm against the logarithm of sample concentration (Fig. S6).
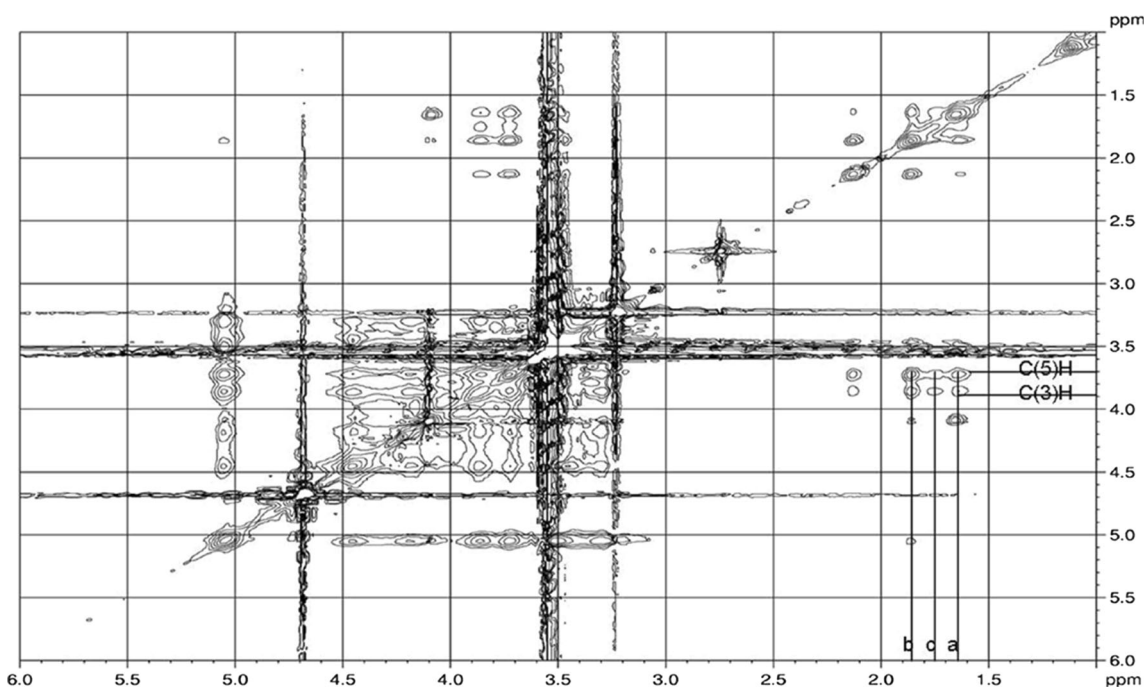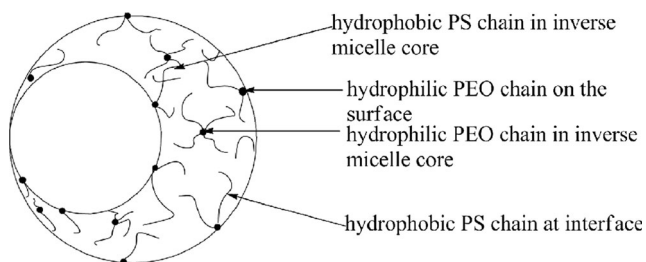

Fig. 1 The ROESY NMR spectrum of a 2:1 mixture β-CD-PEO and AD-PS-AD moieties

Table 2 Materials, preparative conditions, and morphological characteristics of bowl-shaped structures

Triblock copolymer	PEO concentration (wt.% in copolymer)	Mn (PS) (g/mol)	Mw/Mn (PS)	Initial concentration in THF (wt.%)	Morphologies
1	32.7	9200	1.17	0.8	Vesicles and bowl-shaped
	32.7	9200	1.17	1.2	LCMs
2	68	12,000	1.11	0.5	Vesicles and bowl-shaped
	68	12,000	1.11	0.6	LCMs

The morphology of the triblock copolymer systems has large compound micelles (LCMs) and porous spheres (Fig. 1). Schematic structure of a cross section of the bowl-shaped aggregates (Fig. 2) shows that the bowl-shaped aggregate have an internal structure similar to that of typical LCM conversion from a good solvent for the PS blocks, in which the blocks form reverse micellics with the polar cores inside and the PS on the corona. The morphology encountered in these triblock copolymer systems is similar to other structures previously encountered in copolymers, which could not be directly dissolved in water [64, 65]. The final morphology appears in the form of the compound micelles or the porous spheres [66].

TEM and SEM micrographs demonstrated bowl-shaped aggregates obtained from PEO-β-CD-AD-PS-AD-β-CD-PEO at initial concentration of 0.8 and 0.5 wt.% in THF solvents (Figs. 3, 4, and 5). In the early stages, the structure of the void spaces formed by a consequence of the self-assembly is apparently homogeneous; the triblock copolymer shows low viscosity and high chain mobility. The formation of the void spaces resembles that encountered in the porous sphere structures. With the addition of water to the THF solution of the copolymers, the organic solvent (THF) is progressively extracted through the surface of the sphere, which may cause the viscosity of the core to rise and the PS blocks to form a hard skin at the periphery of the aggregates. At last, a cavity forms within the core. THF in the interior diffuses out of the cavities faster than the rate at which water diffuses in, the cavities grow and migrate to the surface of the aggregates, causing the formation of bowl-like vesicles. THF in the interior diffuses out of the cavities faster than the rate at which water diffuses in, the cavities were left, and the bubble breaks through the surface to form bowl-shaped aggregate (Fig. 4). The diameters of the bowls are in the range of 240–600 nm, and the diameters of the void space are between 200 and 400 nm. The apparent diameters of the aggregates obtained from TEM and SEM are consistent with dynamic light scattering (DLS) results. DLS measurement was performed on a MalvernZetasizer NanoSize Distributions and Zeta Potential Meter at 25 °C. As shown in Fig. S7, the number-averaged size of assemblies formulated with PEO-β-CD-AD-PS-AD-β-CD-PEO was 365.1 nm and the PDI was 0.195. They revealed that the NP dimensions are in agreement with the ones determined through TEM measurements (332.8 nm). The asymmetry of force makes the bubble moving in the direction of the thinner wall until the bubble breaks through the surface. Hest et al. recently reported that the spherical morphology of micelles can be reengineered via shape transformations triggered by either a change through variation of external stimuli such as temperature or osmotic pressure [67]. They found that polymer vesicles containing a polystyrene high-molecular-weight glassy segment can be forced to undergo shape transformation from a spherical morphology to a bowl-shaped structure [68]. The solvent increases the flexibility of the polymersome membrane; difference in osmotic pressure is the reason of morphology transformation. After complete removal of the solvent, the polystyrene segments in the membrane recover their rigidity. Bowl-shaped structures' self-propel properties in aqueous media and bowl-shaped stomatocyte architectures show the future prospects for the entrapment of nanosized catalysts, nanoparticles, or other guest molecules. The schematic diagram of the latter is presented in Fig. 5.

Fig. 2 Schematic structure of a cross section of the bowl-shaped aggregates

Labels: hydrophobic PS chain in inverse micelle core; hydrophilic PEO chain on the surface; hydrophilic PEO chain in inverse micelle core; hydrophobic PS chain at interface

Conclusion

In summary, we have studied the morphologies and the vesicle formation of a self-assemble noncovalent dumbbell-shaped amphiphilic triblock copolymer, which was prepared through the host–guest interactions between β-cyclodextrin modified poly(ethylene oxide) (β-CD-PEO) and adamantane-

Fig. 3 TEM picture of the bowl-shaped structures from the triblock copolymer: the bubble to break through the surface. **a** PEO concentration 32.7 wt.%, Mn (PS)=9200 g/mol, Mw/Mn (PS)=1.17, initial concentration in THF (wt.%)=0.8. **b** PEO concentration 68 wt.%, Mn (PS)= 12,000 g/mol, Mw/Mn (PS)= 1.11, initial concentration in THF (wt.%)=0.5. **c** PEO concentration 32.7 wt.%, Mn (PS)=9200 g/mol, Mw/Mn (PS)=1.17, initial concentration in THF (wt.%)=0.8
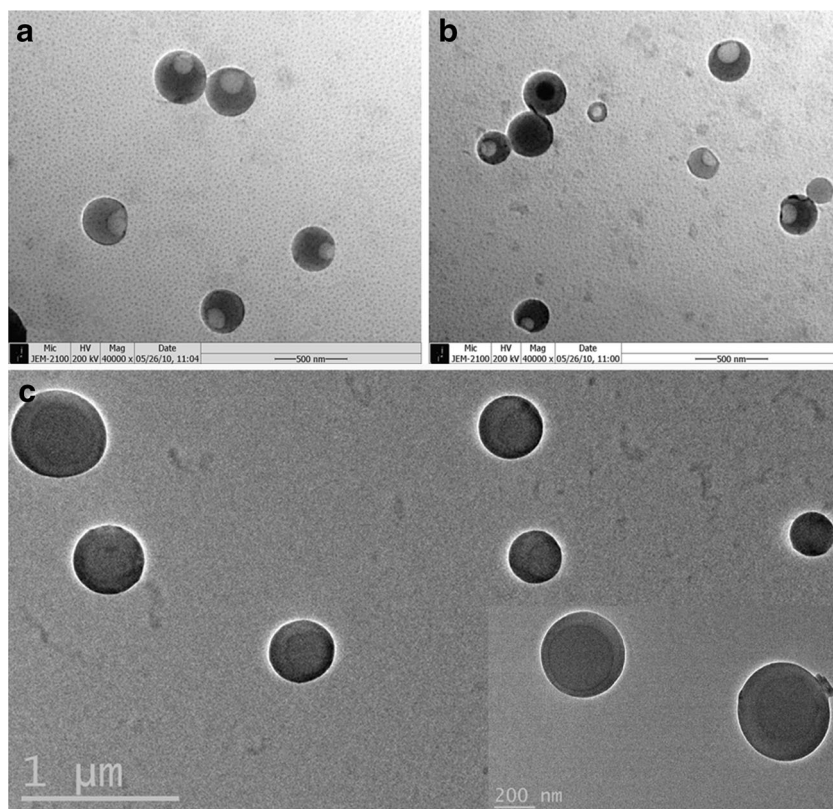
polystyrene-adamantane (AD-PS-AD) in a dilute solution. The normal spherical micelles with average diameters of 50 nm and the bowl-shaped aggregates with an average diameter of 300 nm, the concentration of triblock copolymer in

Fig. 4 SEM picture of the triblock copolymer. **a** PEO concentration 32.7 wt.%, Mn (PS)=9200 g/mol, Mw/Mn (PS)=1.17, initial concentration in THF (wt.%)=0.8. **b** PEO concentration 68 wt.%, Mn (PS)= 12,000 g/mol, Mw/Mn (PS)= 1.11, initial concentration in THF (wt.%)=0.5. **c** PEO concentration 32.7 wt.%, Mn (PS)=9200 g/mol, Mw/Mn (PS)=1.17, initial concentration in THF (wt.%)= 0.8. **d** PEO concentration 68 wt.%, Mn (PS)=12,000 g/mol, Mw/Mn (PS)=1.11, initial concentration in THF (wt.%)=0.5
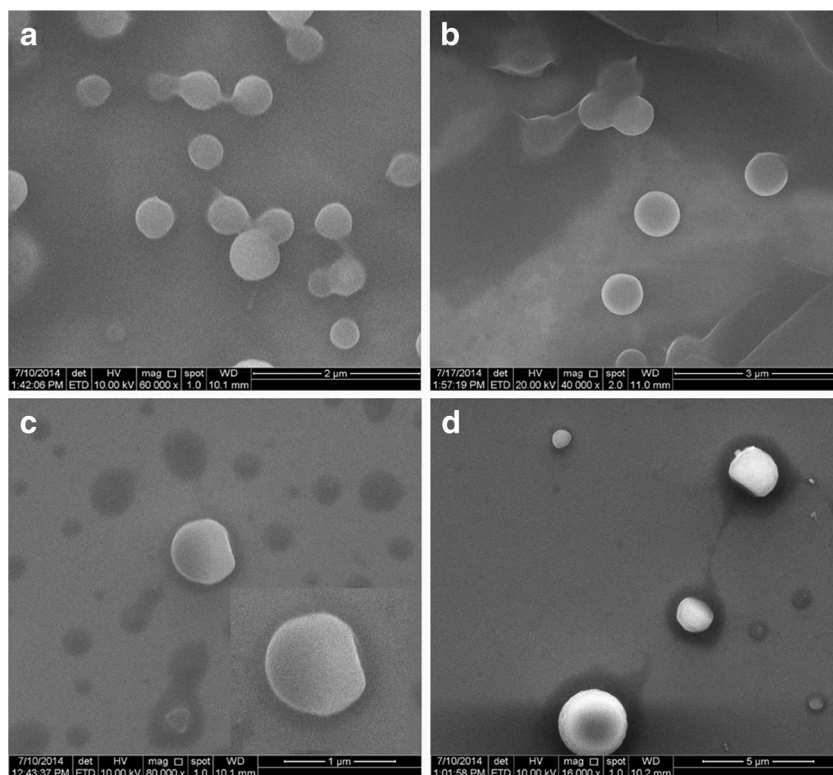
Fig. 5 The schematic diagram of the move of the single large bubble

THF, and concentration of hydrophilic group (PEO) are key factors of different morphologies. The bowl-shaped morphologies and the vesicle formation in this system could be ascribed to LCMs and porous spheres.

References

1. Patra D, Huang T-Y, Chiang C-C, Maturana ROV, Pao C-W, Ho K-C, Wei K-H, Chu C-W (2013) 2-alkyl-5-thienyl-substituted benzo 1,2-b:4,5-b′ dithiophene-based donor molecules for solution-processed organic solar cells. ACS Appl Mater Interfaces 5:9494–9500

2. Swiergiel J, Bouteiller L, Jadzyn J (2014) Concentration evolution of the dielectric response of hydrogen-bonded supramolecular polymers formed by dialkylurea in Non-polar medium. Macromolecules 47:2464–2470

3. Sun X, Lindner J-P, Bruchmann B, Schlueter AD (2014) Synthesis of neutral, water-soluble oligo-ethylene glycol-containing dendronized homo- and copolymers of generations 1, 1.5, 2, and 3. Macromolecules 47:7337–7346

4. Frank PG, Tuten BT, Prasher A, Chao D, Berda EB (2014) Intra-chain photodimerization of pendant anthracene units as an efficient route to single- chain nanoparticle fabrication. Macromol Rapid Commun 35:249–253

5. Binauld S, Stenzel MH (2013) Acid-degradable polymers for drug delivery: a decade of innovation. Chem Commun 49:2082–2102

6. Wen Y, Zhang Z, Li J (2014) Highly efficient multifunctional supramolecular gene carrier system self-assembled from redox-sensitive and zwitterionic polymer blocks. Adv Funct Mater 24: 3874–3884

7. Suzuki M, Hanabusa K (2010) Polymer organogelators that make supramolecular organogels through physical cross-linking and self-assembly. Chem Soc Rev 39:455–463

8. Samanta D, Sarkar A (2011) Immobilization of bio-macromolecules on self-assembled monolayers: methods and sensor applications. Chem Soc Rev 40:2567–2592

9. Chen S, Cheng S-X, Zhuo R-X (2011) Self-assembly strategy for the preparation of polymer-based nanoparticles for drug and gene delivery. Macromol Biosci 11:576–589

10. Oohora K, Onoda A, Kitagishi H, Yamaguchi H, Harada A, Hayashi T (2011) A chemically-controlled supramolecular protein polymer formed by a myoglobin-based self-assembly system. Chem Sci 2:1033–1038

11. Luo Q, Dong Z, Hou C, Liu J (2014) Protein-based supramolecular polymers: progress and prospect. Chem Commun 50:9997–10007

12. Guo J, Zhuang JM, Wang F, Raghupathi KR, Thayumanavan S (2014) Protein AND enzyme gated supramolecular disassembly. J Am Chem Soc 136:2220–2223

13. Tareste D, Pincet F, Lebeau L, Perez E (2007) Hydrophobic forces and hydrogen bonds in the adhesion between retinoid-coated surfaces. Langmuir 23:3225–3229

14. Munteanu M, Choi S, Ritter H (2009) Cyclodextrin-click-cucurbit 6 uril: combi-receptor for supramolecular polymer systems in water. Macromolecules 42:3887–3891

15. Lu J, Mirau PA, Shin ID, Nojima S, Tonelli AE (2002) Molecular motions in the supramolecular complexes between poly(epsilon-caprolactone)-poly(ethylene oxide)-poly(epsilon-caprolactone) and alpha- and gamma-cyclodextrins. Macromol Chem Phys 203: 71–79

16. Trellenkamp T, Ritter H (2010) Poly(N-vinylpyrrolidone) bearing covalently attached cyclodextrin via click-chemistry: synthesis, characterization, and complexation behavior with phenolphthalein. Macromolecules 43:5538–5543

17. Paolino M, Ennen F, Lamponi S, Cernescu M, Voit B, Cappelli A, Appelhans D, Komber H (2013) Cyclodextrin-adamantane host-guest interactions on the surface of biocompatible adamantyl-modified glycodendrimers. Macromolecules 46:3215–3227

18. Zhang JX, Ma PX (2013) Cyclodextrin-based supramolecular systems for drug delivery: recent progress and future perspective. Adv Drug Deliv Rev 65:1215–1233

19. Srinivasachari S, Reineke TM (2009) Versatile supramolecular pDNA vehicles via "click polymerization" of beta-cyclodextrin with oligoethyleneamines. Biomaterials 30:928–938

20. Jazkewitsch O, Mondrzyk A, Staffel R, Ritter H (2011) Cyclodextrin-modified polyesters from lactones and from bacteria: an approach to new drug carrier systems. Macromolecules 44: 1365–1371

21. Dong H, Li Y, Cai S, Zhuo R, Zhang X, Liu L (2008) A facile one-pot construction of supramolecular polymer micelles from alpha-cyclodextrin and poly(epsilon-caprolactone). Angew Chem Int Ed 47:5573–5576

22. Eftink MR, Andy ML, Bystrom K, Perlmutter HD, Kristol DS (1989) Cyclodextrin inclusion complexes: studies of the variation in the size of alicyclic guests. J Am Chem Soc 111:6765–6772

23. Yhaya F, Lim J, Kim Y, Liang M, Gregory AM, Stenzel MH (2011) Development of micellar novel drug carrier utilizing temperature-sensitive block copolymers containing cyclodextrin moieties. Macromolecules 44:8433–8445

24. Dimitrov P, Iyer P, Bharadwaj R, Mallya P, Hogen-Esch TE (2009) Controlled synthesis of high molecular weight polyacrylates having a dumbbell topology. Macromolecules 42:6873–6877

25. Liang S, Claude J, Xu K, Wang Q (2008) Synthesis of dumbbell-shaped triblock structures containing ferroelectric polymers and oligoanilines with high dielectric constants. Macromolecules 41: 6265–6268

26. Nuhn L, Schull C, Frey H, Zentel R (2013) Combining ring-opening multibranching and RAFT polymerization: multifunctional linear-hyperbranched block copolymers via hyperbranched macro-chain-transfer agents. Macromolecules 46:2892–2904

27. Schmidt BVKJ, Hetzer M, Ritter H, Barner-Kowollik C (2011) Cyclodextrin-complexed RAFT agents for the ambient temperature aqueous living/controlled radical polymerization of acrylamido monomers. Macromolecules 44:7220–7232

28. Warren NJ, Muise C, Stephens A, Armes SP, Lewis AL (2012) Near-monodisperse poly(2-(methacryloyloxy)ethyl phosphorylcholine)-based macromonomers prepared by atom transfer radical polymerization and thiol-Ene click chemistry: novel reactive steric stabilizers for aqueous emulsion polymerization. Langmuir 28:2928–2936

29. Ohno S, Matyjaszewski K (2006) Controlling grafting density and side chain length in poly(n-butyl acrylate) by ATRP copolymerization of macromonomers. J Polym Sci A Polym Chem 44:5454–5467

30. Giacomelli FC, Riegel IC, Petzhold CL, da Silveira NP, Stepanek P (2009) Aggregation behavior of a new series of ABA triblock copolymers bearing short outer a blocks in B-selective solvent: from free chains to bridged micelles. Langmuir 25:731–738

31. Huo F, Gao CQ, Dan MH, Xiao X, Su Y, Zhang WQ (2014) Seeded dispersion RAFT polymerization and synthesis of well-defined ABA triblock copolymer flower-like nanoparticles. Polym Chem 5:2736–2746

32. Yao J, Ruan Y, Zhai T, Guan J, Tang G, Li H, Dai S (2011) ABC block copolymer as "smart" pH-responsive carrier for intracellular delivery of hydrophobic drugs. Polymer 52:3396–3404

33. Huo F, Li ST, He X, Shah SA, Li QL, Zhang WQ (2014) Disassembly of block copolymer vesicles into nanospheres through vesicle mediated RAFT polymerization. Macromolecules 47: 8262–8269

34. Cai Y, Aubrecht KB, Grubbs RB (2011) Thermally induced changes in amphiphilicity drive reversible restructuring of assemblies of ABC triblock copolymers with statistical polyether blocks. J Am Chem Soc 133:1058–1065

35. Yang YQ, Lin WJ, Zhao B, Wen XF, Guo XD, Zhang LJ (2012) Synthesis and physicochemical characterization of amphiphilic triblock copolymer brush containing pH-sensitive linkage for oral drug delivery. Langmuir 28:8251–8259

36. Wang C-H, Hwang Y-S, Chiang P-R, Shen C-R, Hong W-H, Hsiue G-H (2012) Extended release of Bevacizumab by thermosensitive biodegradable and biocompatible hydrogel. Biomacromolecules 13:40–48

37. Rao J, Luo Z, Ge Z, Liu H, Liu S (2007) "Schizophrenic" micellization associated with coil-to-helix transitions based on polypeptide hybrid double hydrophilic rod-coil diblock copolymer. Biomacromolecules 8:3871–3878

38. Krieg E, Weissman H, Shimoni E, On AB, Rybtchinski B (2014) Understanding the effect of fluorocarbons in aqueous supramolecular polymerization: ultrastrong noncovalent binding and cooperativity. J Am Chem Soc 136:9443–9452

39. Watson SMD, Galindo MA, Horrocks BR, Houlton A (2014) Mechanism of formation of supramolecular DNA-templated polymer nanowires. J Am Chem Soc 136:6649–6655

40. Jimenez A, Bilbeisi RA, Ronson TK, Zarra S, Woodhead C, Nitschke JR (2014) Selective encapsulation and sequential release of guests within a self-sorting mixture of three tetrahedral cages. Angew Chem Int Ed 53:4556–4560

41. Li Z, Ma J, Lee NS, Wooley KL (2011) Dynamic cylindrical assembly of triblock copolymers by a hierarchical process of covalent and supramolecular interactions. J Am Chem Soc 133:1228–1231

42. Wu X, Lin J, Yu DF, Wang JB, Yang H, Su YZ, Ma AQ, Sun KJ, Chen YB (2015) Transformation of self- assembled structures from spherical aggregates in solution to a network structure on a two-dimensional surface. J Appl Polym Sci 132:41945

43. Kedracki D, Chekini M, Maroni P, Schlaad H, Nardin C (2014) Synthesis and self-assembly of a DNA molecular brush. Biomacromolecules 15:3375–3382

44. Liu H, Hsu CH, Lin ZW, Shan WP, Wang J, Jiang J, Huang MJ, Lotz B, Yu XF, Zhang WB, Yue K, Cheng SZD (2014) Two-dimensional nanocrystals of molecular janus particles. J Am Chem Soc 136:10691–10699

45. Yan Q, Zhao Y (2014) Block copolymer self-assembly controlled by the "green" gas stimulus of carbon dioxide. Chem Commun 50: 11631–11641

46. Li XX, Yang YH, Li GJ, Lin SL (2014) Synthesis and self-assembly of a novel fluorinated triphilic block copolymer. Polym Chem 5:4553–4560

47. Gwyther J, Gilroy JB, Rupar PA, Lunn DJ, Kynaston E, Patra SK, Whittell GR, Winnik MA, Manners I (2013) Dimensional control of block copolymer nanofibers with a π-conjugated core: crystallization-driven solution self-assembly of amphiphilic poly(3-hexylthiophene)-b-poly(2-vinylpyridine). Chem Eur J 19: 9186–9197

48. Wang LQ, Lin JP, Zhang X (2013) Hierarchical microstructures self-assembled from polymer systems. Polymer 54:3427–3442

49. Cai C, Wang L, Lin J, Zhang X (2012) Morphology transformation of hybrid micelles self-assembled from rod-coil block copolymer and nanoparticles. Langmuir 28:4515–4524

50. Greenall MJ, Schuetz P, Furzeland S, Atkins D, Buzza DMA, Butler MF, McLeish TCB (2011) Controlling the self-assembly of binary copolymer mixtures in solution through molecular architecture. Macromolecules 44:5510–5519

51. Schmidt V, Borsali R, Giacomelli C (2009) Aggregation of a versatile triblock copolymer into pH-responsive cross-linkable nanostructures in both organic and aqueous media. Langmuir 25:13361–13367

52. Menon S, Thekkayil R, Varghese S, Das S (2011) Photoresponsive soft materials: synthesis and photophysical studies of a stilbene-based diblock copolymer. J Polym Sci A Polym Chem 49:5063–5073

53. Walther A, Goldmann AS, Yelamanchili RS, Drechsler M, Schmalz H, Eisenberg A, Mueller AHE (2008) Multiple morphologies, phase transitions, and cross-linking of crew-cut aggregates of poly-butadiene-block-poly(2-vinylpyridine) diblock copolymers. Macromolecules 41:3254–3260

54. Burkhardt M, Martinez-Castro N, Tea S, Drechsler M, Babin I, Grishagin I, Schweins R, Pergushov DV, Gradzielski M, Zezin AB, Mueller AHE (2007) Polyisobutylene-block-poly(methacrylic acid) diblock copolymers: self-assembly in aqueous media. Langmuir 23:12864–12874

55. Lund R, Willner L, Pipich V, Grillo I, Lindner P, Colmenero J, Richter D (2011) Equilibrium chain exchange kinetics of diblock copolymer micelles: effect of morphology. Macromolecules 44: 6145–6154

56. Lauw Y, Leermakers FAM, Stuart MAC, Borisov OV, Zhulina EB (2006) Coexistence of crew-cut and starlike spherical micelles composed of copolymers with an annealed polyelectrolyte block. Macromolecules 39:3628–3641

57. Zhang M, Wang M, He S, Qian J, Saffari A, Lee A, Kumar S, Hassan Y, Guenther A, Scholes G, Winnik MA (2010) Sphere-to-wormlike network transition of block copolymer micelles containing CdSe quantum dots in the corona. Macromolecules 43:5066–5074

58. LaRue I, Adam M, Zhulina EB, Rubinstein M, Pitsikalis M, Hadjichristidis N, Ivanov DA, Gearba RI, Anokhin DV, Sheiko SS (2008) Effect of the soluble block size on spherical diblock copolymer micelles. Macromolecules 41:6555–6563

59. Zhulina EB, Adam M, LaRue I, Sheiko SS, Rubinstein M (2005) Diblock copolymer micelles in a dilute solution. Macromolecules 38:5330–5351

60. Burke SE, Eisenberg A (2001) Kinetics and mechanisms of the sphere-to-rod and rod-to-sphere transitions in the ternary system PS310-b-PAA(52)/dioxane/water. Langmuir 17:6705–6714

61. Petrov PD, Drechsler M, Mueller AHE (2009) Self-assembly of asymmetric poly(ethylene oxide)-block-poly (n-butyl acrylate) diblock copolymers in aqueous media to unexpected morphologies. J Phys Chem B 113:4218–4225

62. Riegel IC, Eisenberg A, Petzhold CL, Samios D (2002) Novel bowl-shaped morphology of crew-cut aggregates from amphiphilic block copolymers of styrene and 5-(N, N-diethylamino)isoprene. Langmuir 18:3358–3363

63. Liu XY, Kim JS, Wu J, Eisenberg A (2005) Bowl-shaped aggregates from the self-assembly of an amphiphilic random copolymer of poly(styrene-co-methacrylic acid). Macromolecules 38:6749–6751

64. Liu X, Liu J, Jiang M (2009) Spontaneous self-assembly of a mono-component polyimide bearing terminal hydrogen-bonding sites in a single solvent. Macromol Rapid Commun 30:892–896

65. Wang J, Kuang M, Duan HW, Chen DY, Jiang M (2004) pH-dependent multiple morphologies of novel aggregates of carboxyl-terminated polyimide in water. Eur Phys J E 15:211–215

66. Zhang Y, Zhao C, Liu L, Zhao H (2013) Polymeric micelles with mesoporous cores. ACS Macro Lett 2:891–895

67. Wilson DA, Nolte RJM, van Hest JCM (2012) Entrapment of metal nanoparticles in polymer stomatocytes. J Am Chem Soc 134:9894–9897

68. Kim KT, Zhu J, Meeuwissen SA, Cornelissen JJLM, Pochan DJ, Nolte RJM, van Hest JCM (2010) Polymersome stomatocytes: controlled shape transformation in polymer vesicles. J Am Chem Soc 132:12522–12524